Journal of Hazardous Materials 191 (2011) 49–55

Contents lists available at ScienceDirect

Journal of Hazardous Materials

journal homepage: www.elsevier.com/locate/jhazmat

The efficiency of CO_2 sequestration via carbonate mineralization with simulated wastewaters of high salinity

S. Mignardi [a,*], C. De Vito [a], V. Ferrini [a], R.F. Martin [b]

[a] Dipartimento di Scienze della Terra, Sapienza Università di Roma, P.le Aldo Moro 5, I-00185 Roma, Italy
[b] Department of Earth and Planetary Sciences, McGill University, 3450 University Street, Montreal, QC H3A 2A7, Canada

ARTICLE INFO

Article history:
Received 20 December 2010
Received in revised form 6 April 2011
Accepted 7 April 2011
Available online 27 April 2011

Keywords:
Solubility of CO_2
Carbonate mineralization
Nesquehonite
Carbon dioxide sequestration
Discharge of saline wastewater

ABSTRACT

Salinity generally strongly affects the solubility of carbon dioxide in aqueous solution. This would seem to involve a reduction of the efficiency of the carbonate mineralization process with the objective to sequester this greenhouse gas. On the contrary, we demonstrate here that with a more concentrated solution of magnesium chloride, the residence time of CO_2 is enhanced in the aqueous medium because of a reduced tendency to produce $CO_{2(g)}$. Experiments intended to simulate more closely the Mg-rich wastewaters that are industrially available have been carried out using solutions differing in Mg concentration (7, 16, 32 g L^{-1} Mg). A comparison of the efficiency of the CO_2 mineralization process among sets of experiments shows that the reduction of the efficiency, to about 65%, was lower than that expected, as the low degree of CO_2 degassing results in the enhanced availability of carbonic ions to react with Mg ions to form stable carbonate minerals over a longer time.

1. Introduction

Emissions of carbon dioxide due to anthropogenic activities continue to be a source of major environmental concern [1–4]. Many groups are actively seeking practical ways to sequester CO_2 being produced industrially, to prevent it from worsening the present alarming situation. Those approaches based on "CO_2 mineralization" offer an attractive option for the permanent and safe storage of a solid carbonate [5–14]. Our group has recently described a carbonation process involving the reaction of gaseous CO_2 bubbling through a magnesium chloride solution; we have shown that the precipitate, a low-temperature phase called nesquehonite, of composition $MgCO_3 \cdot 3H_2O$, efficiently removed a major proportion of the CO_2 being bubbled through the reaction column [15,16]. Nesquehonite occurs in nature as a low-temperature mineral, and the synthetic product can profitably be used in a large number of industrial applications, for example, in the production of ecocement and corrosion-resistant protective coatings [17,18].

Our initial work [15] on the nesquehonite project involved a relatively dilute solution of magnesium chloride, roughly 7 g L^{-1} of Mg, created by dissolving analytical grade $MgCl_2 \cdot 6H_2O$ in water at room temperature. The reaction rate was found to be rapid, the deposition of nesquehonite being virtually complete in about ten minutes. The precipitate removed over 80% of the carbon dioxide in solution, and the pH of the solution, adjusted by adding ammonia, was made to range at an optimum value between 7.8 and 8.2.These experiments were carried out using Mg concentrations of the solutions about 1/10 of the readily available saline wastewater (e.g., produced water, PW).

The application of the nesquehonite approach to CO_2 sequestration has several advantages: the process is kinetically favoured and simple, the precipitate is of high purity, it forms in a very short time, the reactants are locally abundant, nesquehonite can be used for industrial purposes, and its disposal near the surface or underground involves limited environmental risks. Indeed, Ballirano et al. [16] demonstrated that the storage of nesquehonite requires no monitoring up to 373 K; beyond that temperature, the transformation to magnesite, a carbonate thermally stable up to ~600 K, ensures a safe encapsulation of CO_2 for millions of years.

Those encouraging results have led to additional experiments intended to simulate more closely the Mg-rich wastewaters that are industrially available. For example, water produced as a by-product of oil and gas production contains close to ten times the concentration of magnesium chloride in our initial solution. Obvious questions arise. What is the effect of such high concentrations of the reactant on the rate of nesquehonite precipitation? Are there chloride-bearing phases being coprecipitated that adversely affect the efficiency of the sequestration of CO_2? We have found little direct information on the behaviour of CO_2 in such concentrated Mg chloride brines in the literature [19].

It is known that the degree to which CO_2 dissolves in water is determined by the solubility constant $K_0 = [CO_2{}^*]/[CO_{2(g)}]$, where

* Corresponding author. Tel.: +390 649914836; fax: +390 64454729.
E-mail address: silvano.mignardi@uniroma1.it (S. Mignardi).

0304-3894/$ – see front matter © 2011 Elsevier B.V. All rights reserved.
doi:10.1016/j.jhazmat.2011.04.030

$CO_2{}^*$ is the sum of the species $CO_{2(aq)}$ and $H_2CO_{3(aq)}$ [20]. The constant K_0 depends on temperature, pressure, salinity and the ionic composition of the water: increasing temperature favours the gas phase and shifts reaction (1) to the left, as will an increase in salinity of the electrolyte solution, whereas increasing pressure results in higher solubility of CO_2.

$$CO_{2(g)} = CO_{2(aq)} \quad (1)$$

Moreover, the presence of different salts in the solution can be expected to reduce the solubility of CO_2 in the solution. This decrease in $[CO_2{}^*]$ due to salinity is known as the "salting out effect" [21,22]: the solubility of the non-electrolyte (in this case, CO_2) in H_2O is expected to decrease as electrolyte is added. In this case, adding large quantities of $MgCl_2$ creates a network of hydrogen bonds with H_2O molecules that shifts the equilibria (1) and (2) toward the left.

$$CO_{2(aq)} + H_2O_{(l)} = H_2CO_{3(aq)} \quad (2)$$

This reduction in the solubility of CO_2 would seem at first glance to reduce the efficiency of the carbonate mineralization process. In fact, we demonstrate in this paper that with a more concentrated solution of magnesium chloride, the residence time of CO_2 is enhanced in the aqueous medium because of a reduced tendency to produce $CO_{2(g)}$. At equivalent CO_2 contents, the more saline the solution, the less effective is the loss of the gas phase. Because of the stabilization of the level of dissolved CO_2, nesquehonite could be expected to form in lower quantities but over a longer period of time compared to an equivalent volume of the more dilute electrolyte solution. However, this apparent drawback will be compensated by the decrease in the degassing of CO_2 and by the use of a single electrolyte in the reacting solution.

The dissociation constants K_1 and K_2, which refer to the first and second dissociation of carbonic acid [Eqs. (3) and (4), respectively] are similarly dependent on temperature and the ionic composition of aqueous medium.

$$H_2CO_{3(aq)} = H^+ + HCO_3{}^-{}_{(aq)} \quad (3)$$

$$HCO_3{}^-{}_{(aq)} = H^+ + CO_3{}^{2-}{}_{(aq)} \quad (4)$$

In the carbonation reactions considered important in CO_2 sequestration, the ionization fraction α, or the relative proportion of species of inorganic carbon present in solution, drives which proportion of species of inorganic carbon will re-ionize to CO_2. In solutions having high salinity, a larger fraction of the carbonic species will reform CO_2 than in low-salinity solutions at equivalent CO_2 contents [20]. In the case of a carbonation process intended to sequester CO_2 in mineral structures, any reduction of the amount of CO_2 due to degassing results in a change in the concentration of ionic species able to react with the available cations to form carbonate minerals. Furthermore, the rate of dehydroxylation of $HCO_3{}^-$ to CO_2 is known to be a slow process [23,24], such that in solutions of high salinity, this reaction will contribute little to a degassing reaction. The low degree of CO_2 degassing in the Mg chloride solution thus enhances the reaction of carbonic ions, whose availability is fixed by the ionization fraction, with Mg ions to form stable carbonate minerals.

2. Experimental

2.1. Syntheses

The synthesis of hydrated Mg-carbonates has been carried out at room temperature using tap water from Rome (Italy), compressed CO_2 from SAPIO (Italy) and analytical grade reagents [$MgCl_2{\cdot}6H_2O$ and ammonia solution (25%) NH_3, Merck p.a.].

Table 1
Experimental conditions and results of representative experiments.

Sample	Temperature (°C)	Approx. volume of the solution (mL)	Initial Mg ($g\,L^{-1}$)	Flux of CO_2 ($mL\,min^{-1}$)	Run duration (min)	pHi	NH_3 solution (mL)	pH_p	Solid products formed	Weight of solids formed (g)	Mg in the residual solution ($g\,L^{-1}$)	CO_2 captured (%)
AC7	20 ± 2	200	7	100	15	5.2	3.5	7.9	N	7.2	0.32	77.7
AC9	22 ± 2	200	7	100	15	5.4	4.0	8.0	N	7.5	0.34	80.6
AC 11	20 ± 2	200	7	100	15	5.3	3.0	8.1	N	7.1	0.35	76.8
AC12	20 ± 2	200	7	100	15	5.6	3.5	8.2	N	7.5	0.37	81.3
AC13	21 ± 2	200	7	100	15	5.4	3.0	8.2	N	7.6	0.29	82.4
AC15	20 ± 2	7200	16	150	50	6.7	250	8.8	AC	30.2	9.5	74.3[a]
AC15B	20 ± 2	200	9.5	no CO_2 addition		8.7			N	0.5	8.9	–
AC15batch	20 ± 2	200	9.5	150	20	6.2	1.5	8.7	N	11.8	0.79	63.7[b]
AC17	22 ± 2	7200	16	150	50	6.3	240	8.8	AC	29.9	9.1	73.6[a]
AC17batch	22 ± 2	200	9.1	150	20	6.4	2.5	8.9	N	11.6	0.93	62.6[b]
AC18	20 ± 2	3600	32	120	60	6.1	53	8.7	CHL	5.0	30.4	–
AC18B	20 ± 2	200	30.4	no CO_2 addition		8.5			N	19.4		–
AC19A-E batches	21 ± 2	200	30.4	120	30	6.8	2.0	8.7-7.9[d]	N[c]	29.2	0.16	65.7[b]
AC20A-E batches	20 ± 2	200	30.4	120	30	6.7	2.5	8.9-8.1[d]	N	28.3	0.25	63.7[b]
AC21A-E batches	21 ± 2	200	30.4	120	30	6.5	3.0	8.8-7.9[d]	N	28.9	0.21	65.0[b]

Abbreviations: N = nesquehonite; AC = amorphous carbonates; CHL = chlorartinite; pH_i = pH values upon stopping the flux of CO_2 and pH_p = pH values of carbonate precipitation.
[a] Calculated assuming that the amorphous carbonates (AC) have a bulk composition similar to that of dypingite.
[b] Calculated considering only the addition of CO_2 (150 mL min^{-1} for 20 min and 120 mL min^{-1} for 30 min).
[c] Minor amounts (~5 vol.%) of lansfordite also are present in sample AC19C.
[d] pH range recorded after collection of each sample without any adjustment.

In forty-seven experiments, we synthesized carbonates using $MgCl_2{\cdot}6H_2O$ as a source of magnesium and sparging CO_2 through the Mg chloride solution. The time of interaction of the flux of CO_2 with the solution has been prolonged to the point of saturation of the solution in CO_2, as suggested by the stabilization of pH values. The pH (pH_i in Table 1), upon stopping the flux of CO_2, ranged between 5.0 and 6.8.

On the basis of the Mg concentration in the solutions, the experiments can be grouped in three series (Table 1): 7, 16, 32 g L^{-1} of Mg, representing 1/10, 1/4 and 1/2 of the Mg concentration in PW, respectively [25–28].

In the 7 g L^{-1} series, the experimental conditions were: flux of CO_2 100 mL min^{-1} for 15 min; volume of the $MgCl_2{\cdot}6H_2O$ solution 200 mL; temperature 21–22 ± 2 °C; pH (pH_p in Table 1) range of carbonate precipitation 7.8–8.2.

In the 16 g L^{-1} series, the experimental conditions were: flux of CO_2 150 mL min^{-1} for 50 min in a volume of the $MgCl_2{\cdot}6H_2O$ solution of 7200 mL and flux of 150 mL min^{-1} for 20 min in batches (200 mL) of the initial solution; temperature 20–22 ± 2 °C; pH (pH_p in Table 1) range of carbonate precipitation 8.0–8.9.

Finally, the experimental conditions in the 32 g L^{-1} series were: flux of CO_2 120 mL min^{-1} for 60 min in a volume of the $MgCl_2{\cdot}6H_2O$ solution of 3600 mL; flux of 120 mL min^{-1} for 30 min in batches (200 mL) of the initial solution; temperature 20–22 ± 2 °C; pH (pH_p in Table 1) range of carbonate precipitation 8.0–8.9.

The residual solutions of the syntheses performed in volumes of 3600 and 7200 mL, after the precipitation of the solid products, were recycled for other experiments. Indeed, batches of 200 mL have been collected and some of them were allowed to stand for 30 days in a beaker covered with a plastic film without CO_2 addition (e.g., samples AC15B and AC18B in Table 1). In other batches, a further flux of CO_2, 150 mL min^{-1} for 20 min and 120 mL min^{-1} for 30 min, was added and the pH of the solutions was adjusted to 8.8–8.9 with ammonia solution (1.5–3.5 mL).

The solid products were collected by filtration every 5 days in the 30-days interval (e.g., AC19A-E, AC20A-E, etc. in Table 1). The pH of the solution was recorded after collection of each sample without any adjustment.

2.2. Analytical methods

The products of our syntheses were investigated morphologically by scanning electron microscopy (SEM) using a FEI Quanta 400 system operating at 30 kV, equipped with X-ray energy-dispersive spectroscopy (EDS). X-ray powder-diffraction patterns were obtained using a Seifert diffractometer operating at 40 kV and 30 mA. The XRD patterns were recorded from 5° to 60° 2θ at a rate of 0.02° per step and with a counting time of 8 s per step, using Cu Kα radiation.

In situ X-ray powder-diffraction data were collected in step-scan mode over the angular range 5–145° 2θ (Cu Kα), using a step size 0.0219° 2θ and counting time of 1 s. A total of 101 isothermal measurements were carried out over the range 303–803 K with a temperature step of 5 K.

The Mg content in the residual solution was measured by inductively coupled plasma – atomic emission spectrometry (ICP–AES) using a Varian Vista RL CCD simultaneous spectrometer. The detection limit was 0.01 mg Mg L^{-1}, and the analytical error was estimated to be in the order of 3%.

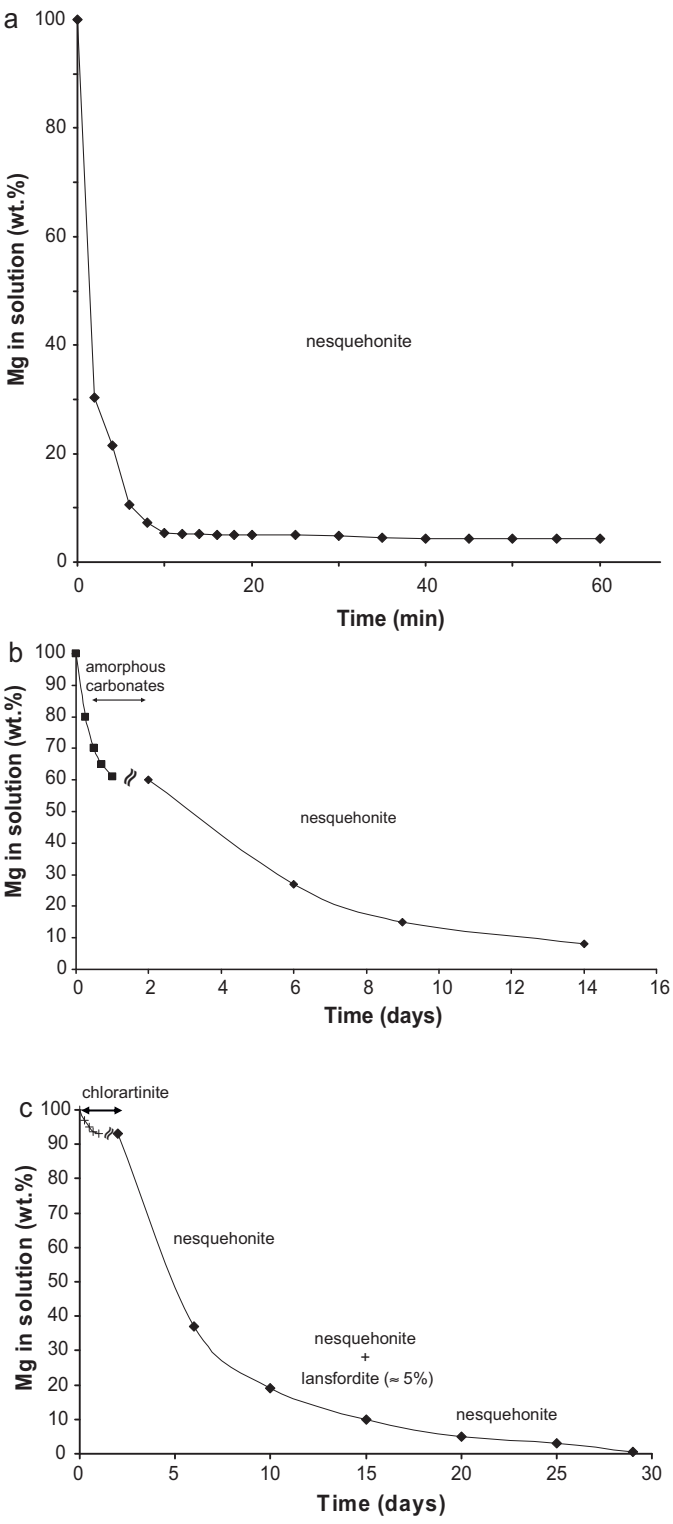

Fig. 1. Kinetics of the carbonation reactions. (a) Experiments performed in solutions having 7 g L^{-1} of Mg showing the rapid formation of nesquehonite; (b) experiments with 16 g L^{-1} of Mg showing the initial precipitation of amorphous carbonates followed by nesquehonite; (c) experiments with 32 g L^{-1} of Mg showing the initial precipitation of chlorartinite followed by nesquehonite with a minor amount of lansfordite.

3. Results

In the experiments of the 7 g L^{-1} of Mg series, the reaction rate was rapid, with carbonate deposition almost complete in about 10 min (Fig. 1a). The XRD patterns of the solid products are in agreement with those reported in JCPDS card 20-669 for nesquehonite in all experiments. The efficiency of the CO_2 mineralization process has been tested by measuring the amount of nesquehonite synthesized and the concentration of Mg in the residual solutions. On the

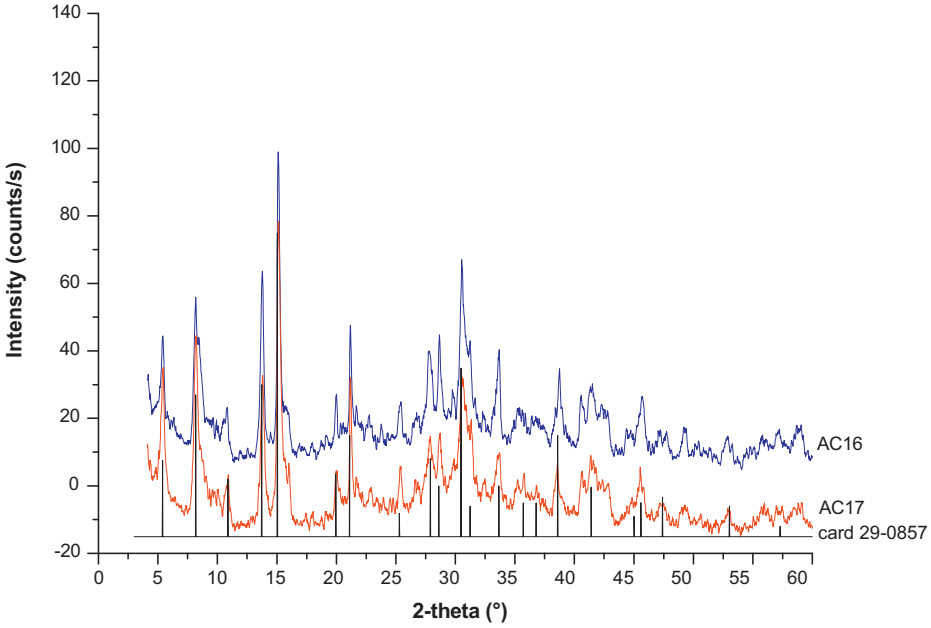

Fig. 2. XRD patterns of synthetic dypingite obtained on samples (AC16 and AC17) stored for at least 5 months in the solution from which they precipitated. The strongest lines recorded in JCPDS card 29-0857 of dypingite have been reported for comparison.

basis of the experimental data, about 80% of the sparged CO_2 was captured to form nesquehonite (Table 1).

With the objective of creating simulations more closely relevant to reality, we performed the synthesis in solutions with higher salinities than in the first series, 16 and finally to 32 g L^{-1} of Mg, representing 1/4 and 1/2 of the Mg concentration in PW, respectively [25–28]. Also, the concentration of CO_2 in the solution and the time of interaction of the flux with the solution have been increased. This resulted in the precipitation of amorphous carbonates in large quantity in the 16 g L^{-1} series (Fig. 1b). In the batches stored without addition of CO_2, there was slow, continuous precipitation of sparse amounts of nesquehonite (e.g., sample AC15B). This finding is confirmed also by the results of ICP–AES analysis, which reveal high concentrations of magnesium in the residual solution.

On the contrary, the addition of CO_2 led to an abundant precipitation of nesquehonite (e.g., samples AC15 batch and AC17 batch) and the reaction efficiency ranged from 62.6 to 63.7%. In the experiments producing amorphous carbonates, the efficiency of the CO_2 mineralization process was calculated on the basis of the weight of the solid products assuming that they were phases with a composition similar to dypingite [$Mg_5(CO_3)_4(OH)_2{\cdot}5H_2O$]. This choice is based on the XRD results obtained on samples stored for at least five months in the solution from which they precipitated (Fig. 2). The percentages of CO_2 captured are reported in Table 1.

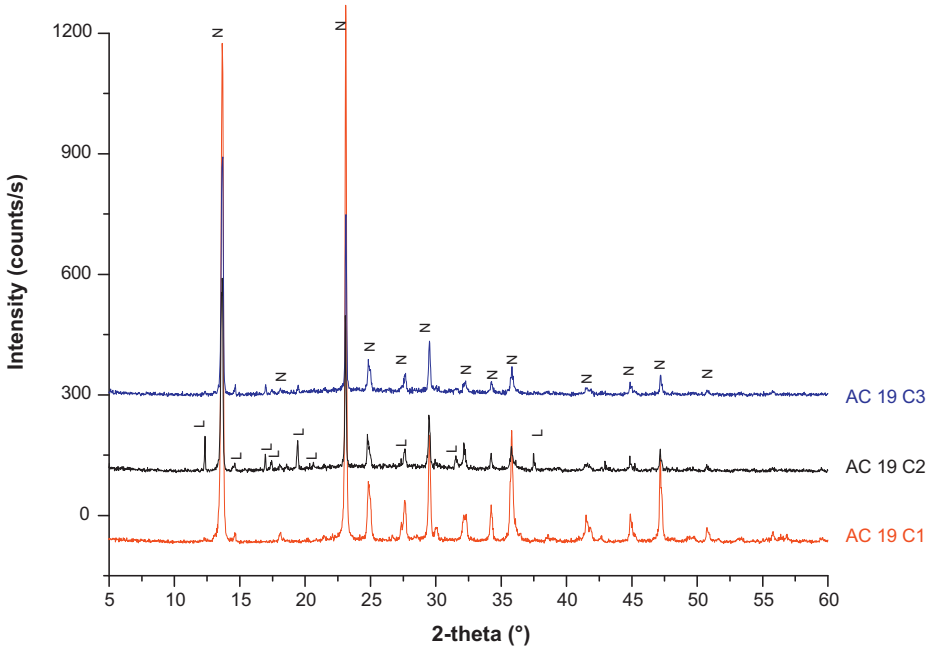

Fig. 3. XRD patterns of synthetic carbonates of the sample AC19C of the batches of AC19A-E. AC19C1 crystals of rosette-like morphology collected at the bottom of the beaker, AC19C2 needle-like crystals collected at the surface of the solution, AC19C3 needle-like crystals collected at the walls and bottom of the beaker. N = nesquehonite and L = lansfordite.

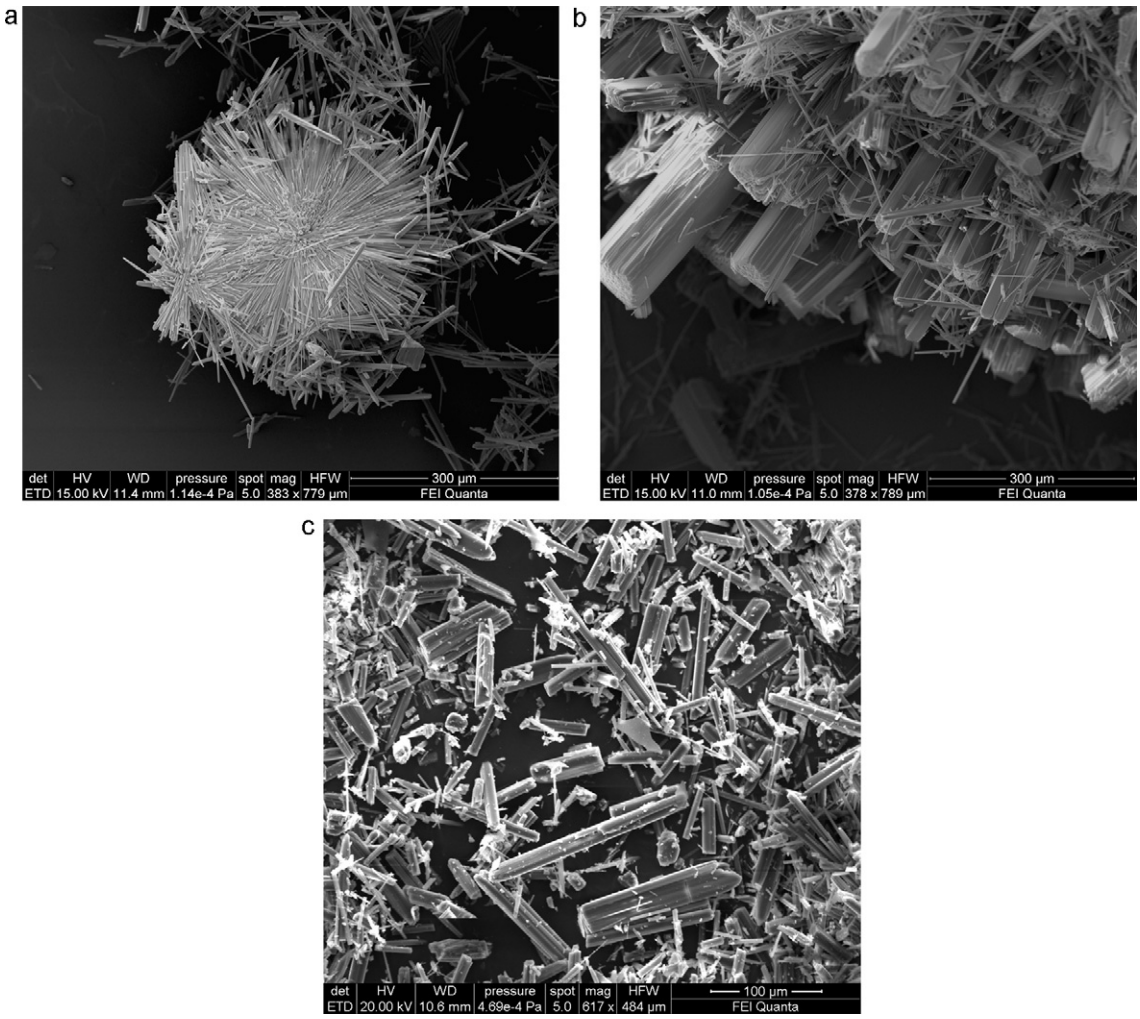

Fig. 4. SEM images of nesquehonite. (a) Rosette-like morphology of interconnected crystals that grew *in situ*; (b) rosette-like morphology at high magnification; (c) needle-like crystals of nesquehonite.

The results of the experiments performed at higher salinity ($32\,g\,L^{-1}$) showed that the precipitation of carbonate minerals occurred continuously for 30 days (Fig. 1c). The first precipitate (sample AC18) exhibits elongate well-formed crystals up to 1 cm in length. The XRD pattern is in good agreement with that of chlorartinite, $Mg_2(CO_3)Cl(OH)\cdot 3H_2O$, as the only precipitate under these conditions. After the initial formation of chlorartinite, in the batches recycled with a further single replenishment of CO_2, crystals continued to precipitate and grow for another 25 days. During this set of experiments, pH values decreased from 8.9 to 7.9 owing to the loss of ammonia during the treatment of the solution.

The XRD patterns of these samples (e.g., AC19A-E, Fig. 3) are in good agreement with those of nesquehonite except for sample AC19C, in which minor amounts (~5 vol.%) of lansfordite, $MgCO_3\cdot 5H_2O$, another carbonate hydrate of magnesium, also are present. The results obtained for other batches (e.g., AC20A-E and AC21A-E) are close to those of the series AC19A-E, except for the formation of lansfordite (Table 1).

Two different morphologies of nesquehonite are observed in all experiments: in general, at the bottom of the beaker, we found a rosette-like morphology of interconnected crystals that grew *in situ* (Fig. 4a), whereas in suspension, the crystals are needle-like (Fig. 4b). Crystal size ranged from 0.5 to 0.6 mm in the samples of the batches in which CO_2 was added (e.g., samples AC19A-E), to 0.7 mm in batches without CO_2 addition (e.g., sample AC18B).

4. Discussion

In the discussion of our experimental results, temperature, pressure and the influence of different salt species in solutions did not affect the process because they were maintained constant. The results of the experiments in more concentrated and more realistic solutions highlight the fact that salinity drives both the kinetics of the process and determines the solid assemblage.

At low concentrations of Mg ($7\,g\,L^{-1}$; Fig. 1a), the rate of reaction was found to be rapid, with nesquehonite deposition almost complete in about 10 min. Conversely, Fig. 1b illustrates that at higher Mg concentration ($16\,g\,L^{-1}$), an abundant yield of an amorphous carbonate hydrate forms in about 24 h. Assuming that the amorphous carbonates have composition similar to the analogue crystalline dypingite (as indicated by XRD patterns obtained on samples stored for at least five months in the solution from which they precipitated), i.e., with a CO_2:Mg ratio lower than nesquehonite, we can infer that the concentration of CO_2 in solution did not allow the precipitation of nesquehonite. Indeed, the addition of CO_2 in the batches of residual solution resulted in the formation of nesquehonite for about two weeks.

The dynamics of the process in more concentrated solutions ($32\,g\,L^{-1}$) are more complicated. In Fig. 1c, we recognize two main steps: (1) chlorartinite precipitation in the first day, (2) nesquehonite formation for about 30 days in the recycled batches with a single replenishment of CO_2. Only in sample AC19C did minor

quantities of lansfordite (<5 vol.%) co-precipitate with nesquehonite. This phase has a CO_2:Mg ratio lower than nesquehonite, and appears only because CO_2 was largely extracted from the system by the early precipitation of abundant nesquehonite.

Our findings show that it is possible to apply our carbonation method to a pilot plant in two different ways, involving solutions of both low and high concentrations of magnesium. In the first case, the synthesis of carbonate minerals is rapid, only nesquehonite forms (Fig. 1a), and there are no drawbacks related to the occurrence of a complex assemblage of mineral phases likely having different fields of thermal stability and structural properties. However, in the likelihood of wastewater having Mg concentration higher than 7 g L^{-1}, should their dilution to the ideal concentration be required, what does one do with the massive volumes of wastewater that would arise from such dilution to 7 g L^{-1}? What is the salinity threshold above which the efficiency of the carbonation process is limited? In this paper, we have explored the second case, involving the use of wastewater having salinity between 16 and 32 g L^{-1}, as their treatment in terms of amounts of waste is relatively lower, and the relative cost is reduced. Clearly, it is necessary to operate in the optimal conditions, taking into consideration the drawbacks of dealing with concentrations of Mg close to or above 32 g L^{-1} (Fig. 1). A comparison between the efficiency of CO_2 mineralization process in all sets of experiments (i.e., 7, 16 and 32 g L^{-1}) shows that the reduction in efficiency was less than expected because the low degree of CO_2 degassing results in a longer-term availability of carbonic ions to react with Mg ions to form stable carbonate minerals.

Wastewater with a salinity in the above range is a byproduct of several industrial processes, such as oil and gas production, and desalination; these activities discharge millions of tonnes each year worldwide [25–30].

The results highlighted here clearly open a new window for the application of our approach to CO_2 sequestration in more concentrated solutions, as reported in Ferrini et al. [15]. The encouraging results demonstrate that the reduced solubility of CO_2 in these more concentrated solutions does not significantly affect the efficiency of the carbonation process. The increased residence-time of carbonic species in solution [Eqs. (3) and (4)] results in a protracted reaction, which will favour the continuous formation of hydrated Mg carbonates. The goal of CO_2 sequestration and management of Mg-rich wastewater seems to be realistically attained also using the more common saline wastewater with limited pretreatment, i.e., reduced dilution. As depicted in Fig. 1, the method can be efficiently applied to wastewater having Mg concentration in the range 7–32 g L^{-1}. We have proven experimentally that in this range of salinity, only carbonate phases formed, including chlorartinite at Mg concentrations greater than about 30 g L^{-1}. However, to avoid the formation of this mineral phase, it is preferable to operate in the salinity range up to 28–30 g L^{-1}, which will favour the formation of high-purity and high-crystallinity nesquehonite. Its thermal and structural stability have been evaluated in view of potential applications to building materials as well as under storage at the temperature conditions prevailing at the Earth's surface.

4.1. CO_2 carbonation via mineralization can contribute to the abatement of aqueous saline waste

The carbonation method proposed by Ferrini et al. [15] was conceived and developed with the double goal of sequestering CO_2 and accommodating the discharge of aqueous waste derived from several industrial processes. The challenge is to consider the saline wastes as a "source" of Mg, to be involved in an industrial process with the objective to mitigate the negative effects of greenhouse gases.

The experimental results of this work have shown that the sequestering of CO_2 by our method can be usefully applied to aqueous saline waste having a salinity up to 30 g L^{-1}. These results suggest that several Mg-rich wastes can be used as reactants in our process. Indeed, the salinity range of the solutions we investigated covers the composition of the more common waste available as sources of Mg for our method (e.g., reject brines and PW). The Mg concentration in the PW ranges between 30 and 60 g L^{-1}; whereas reject brines contain Mg in the range 0.5–20 g L^{-1} [25–29,31]. Huge amounts of PW (about 70 billion barrels each year) and reject brines (about 28 Mm^3/day from seawater sources) are generated worldwide [28,32]. The main constituents of saline waste are inorganic salts in addition to small quantities of additives, corrosion products and pretreatment chemicals [26]. The management and disposal of these saline wastes at the surface of freshwater, streams, ocean, and land application involve environmental concerns due to the contamination of the receiving water, soil and groundwater. This implies pretreatment of this waste to insure the reduction of toxic additives, increase of pH, dilution before their discharge as well as other alternative approaches of remediation [33–35]. According to the ESCWA, the cost of disposing reject brines varies from 5 to 33% of the total cost of the desalination process, depending on the characteristics of the brine, the technology used, the volume of the brine and methodology of disposal [36]. Therefore, alternative mechanisms of disposal and reuse in other industrial processes such as their involvement in the carbonation process must be explored.

Other massive supplies of Mg are the waters of salt lakes and saltpans, such as those occurring in Mexico, China and Turkey, having Mg concentrations in the range 10–50 g L^{-1} [37–39].

5. Conclusions

The results of the experimental work described here suggest that the goal of CO_2 sequestration and Mg-rich wastewater discharge seems to be realistically obtained also using the more common saline wastewater:

1) the method can be efficiently applied to wastewater having Mg concentration in the range 7–32 g L^{-1};
2) the coprecipitation of chloride-bearing carbonates (i.e., chlorartinite) along with hydrated carbonate of Mg (i.e., nesquehonite and rare lansfordite) can be easily avoided using solutions with Mg concentrations lower than 32 g L^{-1}, in the range 28–30 g L^{-1};
3) a CO_2:Mg ratio in solution close to that of nesquehonite (1:1) avoids the precipitation of amorphous carbonates;
4) the reduction in efficiency, to about 65% with respect to about 80% obtained in relatively low-salinity solutions, is lower than expected, as the low degree of CO_2 degassing ensures the availability of carbonic ions to react with Mg ions to form carbonate minerals;
5) this limited reduction in efficiency opens a new window in the application of our method to the discharge of common saline wastewater with limited pre-treatment.

Acknowledgements

Financial support by Sapienza Università di Roma is acknowledged. Additional funding was provided by the Ministry of Education, University and Research (MIUR) through a National Research Program (PRIN 2006045331 001). S.M. and C.D. performed the experimental work, analyzed and interpreted the data and wrote the manuscript with inputs from the other two authors. The authors thank T. Coppola and S. Stellino for the assistance in the ICP-AES and X-ray diffractometer laboratories, respectively. The manuscript benefitted considerably from the insightful and con-

structive comments of JHM reviewers. We are grateful to Gianluca Li Puma for his editorial handling of the manuscript.

References

[1] T. Morita, J. Robinson, A. Adegbulugbe, J. Alcamo, D. Herbert, E.L. Rovere, N. Nakicenovic, H. Pitcher, P. Raskin, K. Riahi, A. Sankovski, V. Sololov, H.J.M. Vries, Z. Dadi, Greenhouse gas emission mitigation scenarios and implications, in: B. Metz, O. Davidson, R. Swart, J. Pan (Eds.), Climate Change 2001: Mitigation, Contribution of Working Group III to the Third Assessment Report of the Intergovernmental Panel on Climate Change, Cambridge University Press, Cambridge, 2001, pp. 115–166.

[2] B. Metz, O. Davidson, H. de Coninck, M. Loos, L. Meyer, (Eds.), Carbon dioxide capture and storage, IPCC Special Report, Cambridge University Press, Cambridge, 2005, pp. 1–433.

[3] IEA, International Energy Agency, The reduction of greenhouse gas emissions from the cement industry. Report No. PH3/7, 1999.

[4] IEA, International Energy Agency. Tracking Industrial Energy Efficiency and CO_2 Emissions. Report ISBN 978-92-64-03016-9, 2007, pp. 324.

[5] K.S. Lackner, D.P. Butt, C.H. Wendt, H.J. Ziock, Mineral carbonates as carbon dioxide sinks, LANL Internal Report. LA-UR-98-4530, 1998.

[6] M. Fernández Bertos, S.J.R. Simons, C.D. Hills, P.J. Carey, A review of accelerated carbonation technology in the treatment of cement-based materials and sequestration of CO_2, J. Hazard. Mater. 112 (2004) 193–205.

[7] D. Georgiou, P.D. Petrolekas, S. Hatzixanthis, A. Aivasidis, Absorption of carbon dioxide by raw and treated dye-bath effluents, J. Hazard. Mater. 144 (2007) 369–376.

[8] E. Rendek, G. Ducom, P. Germain, Carbon dioxide sequestration in municipal solid waste incinerator (MSWI) bottom ash, J. Hazard. Mater. 128 (2006) 73–79.

[9] I.M. Power, S.A. Wilson, J.M. Thom, G.M. Dipple, J.E. Gabites, G. Southam, The hydromagnesite playas of Atlin, British Columbia, Canada: a biogeochemical model for CO_2 sequestration, Chem. Geol. 206 (2009) 302–316.

[10] W.K. O'Connor, D.C. Dahlin, G.E. Rush, C.L. Dahlin, W.K. Collins, Carbon dioxide sequestration by direct mineral carbonation: process mineralogy of feed and products, Miner. Metall. Proc. 19 (2002) 95–101.

[11] D. Daval, I. Martinez, J. Corvisier, N. Findling, B. Goffé, F. Guyot, Carbonation of Ca-bearing silicates, the case of wollastonite: experimental investigations and kinetic modelling, Chem. Geol. 265 (2009) 63–78.

[12] F. Dufaud, I. Martinez, S. Shilobreeva, Experimental study of Mg-rich silicates carbonation at 400 and 500 °C and 1 kbar, Chem. Geol. 265 (2009) 79–87.

[13] M.C. Hales, R.L. Frost, W.N. Martens, Thermo-Raman spectroscopy of synthetic nesquehonite—implication for the geosequestration of greenhouse gases, J. Raman Spectrosc. 39 (2008) 1141–1149.

[14] R.L. Frost, M.C. Hales, W.N. Martens, Thermogravimetric analysis of selected group (II) carbonate minerals—implication for the geosequestration of greenhouse gases, J. Therm. Anal. Calorim. 94 (2008) 1–7.

[15] V. Ferrini, C. De Vito, S. Mignardi, Synthesis of nesquehonite by reaction of gaseous CO_2 with Mg chloride solution: Its potential role in the sequestration of carbon dioxide, J. Hazard. Mater. 168 (2009) 832–837.

[16] P. Ballirano, C. De Vito, V. Ferrini, S. Mignardi, The thermal behaviour and structural stability of nesquehonite, $MgCO_3{\cdot}3H_2O$, evaluated by *in situ* laboratory parallel-beam X-ray powder diffraction: new constraints on CO_2 sequestration within minerals, J. Hazard. Mater. 178 (2010) 522–528.

[17] J. Harrison, Tececo eco-cement masonry product update. http://www.tececo.com.

[18] S.S. Pathak, M.D. Blanton, S.K. Mendon, J.W. Rawlins, Carbonation of Mg powder to enhance the corrosion resistance of Mg-rich primers, Corros. Sci. 52 (2010) 3782–3792.

[19] M. Hänchen, V. Prigiobbe, R. Baciocchi, M. Mazzotti, Precipitation in the Mg-carbonate system-effects of temperature and CO_2 pressure, Chem. Eng. Sci. 63 (2008) 1012–1028.

[20] D. Moran, Carbon dioxide degassing in fresh and saline water. I: degassing performance of a cascade column, Aquacult. Eng. 43 (2010) 29–36.

[21] A. Yasunishi, F. Yoshida, Solubility of carbon dioxide in aqueous electrolyte solutions, J. Chem. Eng. Data 24 (1979) 11–14.

[22] K. Al-Anezi, C. Somerfield, D. Mee, N. Hilal, Parameters affecting the solubility of carbon dioxide in seawater at the conditions encountered in MSF desalination plants, Desalination 222 (2008) 548–571.

[23] W. Stumm, J.J. Morgan, Chemical equilibria and rates in natural waters, in: Aquatic Chemistry, Wiley-Interscience, New York, 1996.

[24] G.R. Grace, R.H. Piedrahita, Carbon dioxide control, in: M.B. Timmons, T.M. Losordo (Eds.), Aquaculture Water Reuse Systems: Engineering Design and Management, Elsevier, New York, 1994, pp. 209–234.

[25] J.A. Veil, M.G. Puder, Regulatory considerations in the management of produced water—a US perspective, Produced Water Management-Gas TIPS (2005) 25–28.

[26] J.A. Veil, M.G. Puder, D. Elcock, R.J. Redweik Jr., A White Paper Describing Produced Water from Production of Crude Oil, Natural Gas, and Coal Bed Methane, United States Department of Energy, National Energy Technology Laboratory, 2004, on-line at http://www.netl.doe.gov/publications/oilpubs/prodwaterpaper.pdf (ContractW-31-109-Eng-8).

[27] J. Lu, X. Wang, B. Shan, X. Li, W. Wang, Analysis of chemical compositions contributable to chemical oxygen demand (COD) of oilfield produced water, Chemosphere 62 (2006) 322–331.

[28] L.E. Kanagy, B.M. Johnson, J.W. Castle, J.H. Rodgers Jr., Design and performance of a pilot-scale constructed wetland treatment system for natural gas storage produced water, Biores. Technol. 99 (2008) 1877–1885.

[29] T. Mezher, H. Fath, Z. Abbas, A. Khaled, Techno-economic assessment and environmental impacts of desalination technologies, Desalination 266 (2010) 263–273.

[30] M. Ahrned, A. Arakel, D. Hoey, M.R. Thumarukudy, M.F.A. Goosen, M. Al-Haddabi, A. Al-Belushi, Feasibility of salt production from inland RO desalination plant reject brine: a case study, Desalination 158 (2003) 109–117.

[31] T. Bleninger, G.H. Jirka, Environmental planning, prediction and management of brine discharges from desalination plants, 2010, MEDRC Series of R&D Reports, MEDRC Project: 07-AS-003.

[32] S. Lattemann, K.H. Mancy, B.S. Damitz, H.K. Khordagui, G. Leslie, Desalination Resource and Guidance Manual for Environmental Impact Assessments. United Nations Environment Programme, S. Lattemann, K.H. Mancy, B.S. Damitz, H.K. Khordagui, G. Leslie (Eds.), Regional Office for West Asia, Manama, and World Health Organization, Regional Office for the Eastern Mediterranean, UNEP 2008, Cairo.

[33] S. Lattemann, T. Höpner, Environmental impact and impact assessment of seawater desalination, Desalination 220 (2008) 1–15.

[34] T. Bleninger, G.H. Jirka, Modelling and environmentally sound management of brine discharges from desalination plants, Desalination 221 (2008) 585–597.

[35] G.H. Jirka, Improved discharge configurations for brine effluents from desalination plants, J. Hydraul. Eng. ASCE 134 (2008) 116–120.

[36] ESCWA (Economic and Social Commission for Western Asia), State of Water Resources in the ESCWA Region, 2007 December Retrieved from, http://www.escwa.un.org/information/publications/edit/upload/sdpd-07-6-e.pdf.

[37] L. Xingqi, H. Dong, J.A. Rech, R. Matsumoto, Y. Bo, W. Yongbo, Evolution of Chaka Salt Lake in NW China in response to climatic change during the Latest Pleistocene–Holocene, Quaternary Sci. Rev. 27 (2008) 867–879.

[38] T.B. Castro, G. Gajardo, J.M. Castro, G.M. Castro, A biometric and ecologic comparison between *Artemia* from Mexico and Chile, Saline Syst. 2 (13) (2006), doi:10.1186/1746-1448-2-13.

[39] Ö. Kilic, A.M. Kilic, Recovery of salt co-products during the salt production from brine, Desalination 186 (2005) 11–19.